Computers & Industrial Engineering 93 (2016) 55–66

Contents lists available at ScienceDirect

Computers & Industrial Engineering

journal homepage: www.elsevier.com/locate/caie

Robust parameter optimization based on multivariate normal boundary intersection

Luiz Gustavo Dias Lopes [b,1], Tarcísio Gonçalves Brito [a,2], Anderson Paulo Paiva [a,2], Rogério Santana Peruchi [a,2], Pedro Paulo Balestrassi [a,*]

[a] UNIFEI – Federal University of Itajuba, Av. BPS, 1303, 37500.188 Itajuba, Minas Gerais, Brazil
[b] FEPI – University Center of Itajubá, Rua Doutor Antonio Braga Filho, 687, 37.501-002 Itajuba, Minas Gerais, Brazil

ARTICLE INFO

Article history:
Received 11 April 2015
Received in revised form 22 December 2015
Accepted 24 December 2015
Available online 4 January 2016

Keywords:
Global optimization
Multivariate statistics
Normal Boundary Intersection (NBI)
Multi-objective Robust Parameter Design (MRPD)
Principal Component Analysis (PCA)

ABSTRACT

Normal Boundary Intersection (NBI) is traditionally used to generate equally spaced and uniformly spread Pareto Frontiers for multi-objective optimization programming (MOP). This method tends to fail, however, when correlated objective functions must be optimized using Robust Parameter Designs (RPD). In such multi-objective optimization programming, there can be reached impractical optima and non-convex frontiers. To reverse this shortcoming, it is common to apply Principal Component Analysis (PCA), which provides uncorrelated objective functions. The aim of this paper is to combine the Robust Parameter Designs, Principal Component Analysis, and Normal Boundary Intersection approaches into a novel method called RPD-MNBI. This approach finds equally spaced Pareto optimal frontiers that are capable of minimizing noise variables' effects. To validate this proposal, this study investigates an end milling process. The most important empirical finding is that the original correlation structure is preserved. On the other hand, the Weighted Sums and Normal Boundary Intersection-Mean Square Error methods, modify the process behavior, resulting in unreal optima. Finally, confirmation runs using an L9 Taguchi design were performed for 10%, 50%, and 90% weights. The proposed method provides process robustness according to confidence intervals for both mean and standard deviation.

1. Introduction

Normal Boundary Intersection (NBI) (Das & Dennis, 1998) was developed mainly to compensate for the shortcomings attributed to the method of weighted sums (WS) in multi-objective optimization programming (MOP). NBI addresses the WS method's inability to find—even when using a uniform spread-of-weight vector—a uniform spread of Pareto optimal solutions. It is possible when using such a vector for there to emerge a non-convex Pareto set with missed Pareto points on the concave parts of the trade-off surface. A pivotal aspect in MOP problems is the presence of strong correlations among the several estimated response surfaces. This aspect of multivariate optimization is very common in the industry and generally promotes unstable regression models and standard errors of coefficients. As a result, the obtained optimization results could be unreal (Bratchell, 1989; Brito, Paiva, Ferreira, Gomes, & Balestrassi, 2014; Govindaluri & Cho, 2007; Jeong, Kim, & Chang, 2005; Kovach & Cho, 2009; Lee & Park, 2006; Paiva et al., 2012; Paiva, Paiva, Ferreira, Balestrassi, & Costa, 2009; Shaibu & Cho, 2009; Shin, Samanlioglu, Cho, & Wiecek, 2011; Tang & Xu, 2002; Wu, 2005; Yuan, Wang, Yu, & Fang, 2008).

To find optimal Pareto solutions, Ahmadi, Moghimi, Esmaeel, Agelidis, and Sharaf (2015) addressed a multi-objective electric model to integrate the generation of thermal units considering heat and power dispatch. To achieve these goals, the researchers employed the NBI method to find the optimal Pareto solution as the best tradeoff between cost, green-house gas emission and heat generation. Aalae, Abderrahmane, Gael, and Olivier (2015) performed a coupling between the NBI algorithm with Radial Basis Function (RBF) to create a simple tool with a reasonable calculation time to solve multi-criteria optimization problems. Their approach was able to efficiently solve the multi-criteria shape optimization problem of structures with nonlinear behavior. Largo, Zhang, and Vega-Rodríguez (2014) applied NBI with a version of the Multi-objective Evolutionary Algorithm based on Decomposition (MOEA/D) for solving tri-objective optimization problems of telecommunication with objectives. The authors argued that their

* Corresponding author. Tel.: +55 35 8877 6958; fax: +55 35 3629 1148.
E-mail addresses: luizgustavo.lopes@yahoo.com.br (L.G.D. Lopes), engtarc.gb@ig.com.br (T.G. Brito), andersonppaiva@unifei.edu.br (A.P. Paiva), rogerioperuchi@gmail.com (R.S. Peruchi), pedro@unifei.edu.br (P.P. Balestrassi).
[1] Tel.: +55 35 3629 8400.
[2] Tel.: +55 35 8877 6958; fax: +55 35 3629 1148.

http://dx.doi.org/10.1016/j.cie.2015.12.023
0360-8352/

List of acronyms

DOE	design of experiment
LCB	lower confidence bound
MNBI	multivariate normal boundary intersection
MOEA/D	Multi-objective Evolutionary Algorithm based on Decomposition
MSE	mean square error
OLS	ordinary least squares
QC	Quality Characteristics
RPD	Robust Parameter Designs
UCB	upper confidence bound
WMMSE	Weighted Multivariate Mean Square Error
DRS	dual response surface
MMSE	multivariate mean square error
MOP	multi-objective optimization programming
MRPD	Multi-objective Robust Parameter Design
NBI	Normal Boundary Intersection
PCA	Principal Component Analysis
RBF	Radial Basis Function
RSM	response surface methodology
WLS	Weighted Least Squares
WS	weighted sums

procedure had shown very promising results in real-world telecommunication problems with multiple objective functions.

In addition to the aforementioned papers, Izadbakhsh, Gandomkar, Rezvani, and Ahmadi (2015) employed the NBI approach to simultaneously minimize the cost and emission for an economic/environmental model for optimal energy management. Oujebbour, Habbal, Ellaia, and Zhao (2014) applied NBI and Normalized Normal Constraint Method to generate a set of Pareto-optimal solution in a MOP problem of a stamping process. Ganesan, Vasant, and Elamvazuthi (2013) used the NBI method to generate optimal solutions to the green sand process. Optimizing multiple responses of rotor-bearing systems, Lopez, Ritto, Sampaio, and de Cursi (2014) came up with a new robust optimization algorithm based on NBI and the penalization of mean and variance for dealing with non-convex MOP.

Given the findings of these papers, it can be seen that the correlation influence becomes more important in the context of Pareto Frontiers. Such an effect should be taken into consideration. Since the procedure weighs two or more objective functions, if the correlation is strong and neglected, the procedure's weights will promote an impractical separation in responses. The natural correlation structure can, as a result of such separation, be highly affected. One could obtain, in other words, an excellent Pareto Frontier composed of unrealistic feasible solutions. To avoid such a Frontier inconsistency, uncorrelated objective functions should be obtained through response surface designs and principal component analyses (PCA). This multivariate technique produces a new dataset, one that extracts eigenvalues and eigenvectors from either a covariance or correlation matrix. It is with the new dataset that uncorrelated response surface models may be built.

Another essential issue in industrial problems is the simultaneous optimization of mean and variance. The combined array is an efficient design of experiment (DOE) approach where the noise variables are inserted into the matrix of control variables, generally represented by a central composite design (Montgomery, 2009). Once the dependent variable (Y) is measured, a full quadratic model, $Y = f(\mathbf{x}, \mathbf{z})$, is estimated by using the ordinary least squares (OLS) algorithm. After that, mean and variance equations can be obtained by taking partial derivatives of the estimated response surface ($\widehat{Y}$) with respect to the noise factors ($\mathbf{z}$).

The noise variables' effect can be expressed as a variance equation. This optimization approach is called Multi-objective Robust Parameter Design (MRPD). The simplest MRPD problem is a bi-objective optimization problem where the two objective functions are the mean and the variance. Suppose now there are ξ estimated models for the mean and the same number of models for the variance. The MOP problem will then have 2ξ estimated equations and ξ dual response surfaces. It thus becomes a non-trivial task to carry out the industrial compromise of offering quality products by employing the simultaneous optimization of blocks of mean and variance equations (Kazemzadeh, Bashiri, Atkinson, & Noorossana, 2008).

This study differs from the most commonly proposed RPD approaches in that the weights of the mean and variance equations of the principal component scores can be obtained from a control-noise response surface equation. Moreover, the weighted approach of principal components has already been used successfully by several authors (Gomes, Paiva, Costa, Balestrassi, & Paiva, 2013; Lopes et al., 2013; Peruchi, Balestrassi, Paiva, Ferreira, & Carmelossi, 2013). Besides reducing dimensions, the RPD-MNBI (robust parameter optimization based on multivariate normal boundary intersection) method has two advantages: (i) It considers the correlation among the multiple responses and (ii) it generates convex Pareto Frontiers of the mean (f_μ) and variance ($f_{\sigma 2}$) functions. Accordingly, this paper presents the RPD-MNBI method, a multi-objective hybrid approach of RPD that couple NBI with PCA for combined arrays while considering the correlation structure among the response variables. To illustrate the proposal, this study uses a case study of a bivariate AISI 1045 steel end milling operation. The optimization results are statistically validated, confirming the adequacy of the paper's proposal.

2. Multi-objective optimization and the NBI technique

Normal Boundary Intersection method (NBI), a MOP procedure developed by Das and Dennis (1998), was intended to compensate for the shortcomings attributed to the WS method. According to Shukla and Deb (2007), the WS approach was unable to come up with a uniform spread of Pareto optimal solutions, even if a uniform spread of weighted vectors had been used. Vahidinasab and Jadid (2010) also found that if the Pareto set was non-convex, the Pareto points on the concave parts of the trade-off surface would be missed. This led to Ganesan et al. (2013) finding that when solving non-convex MOP, the NBI approach was deemed to be a more interesting alternative to the WS method.

To use the NBI method, it is necessary to find the payoff matrix Φ by a calculation based on the individual minimum of each objective function. The solution that minimizes the ith objective function $f_i(x)$ will be denoted by $f_i^*(x_i^*)$. $f_i(x_i^*)$ which is obtained when the individual optimal solution x_i^* is substituted in the objective functions. The payoff matrix Φ is shown in Eq. 1.

$$\Phi = \begin{bmatrix} f_1^*(x_1^*) & \cdots & f_1(x_i^*) & \cdots & f_1(x_m^*) \\ \vdots & \ddots & & & \vdots \\ f_i(x_1^*) & \cdots & f_i^*(x_i^*) & \cdots & f_i^*(x_m^*) \\ \vdots & & & \ddots & \vdots \\ f_m(x_1^*) & \cdots & f_m(x_i^*) & \cdots & f_m^*(x_m^*) \end{bmatrix} \Rightarrow \bar{\Phi} = \begin{bmatrix} \bar{f}_1 & \cdots & \bar{f}_1 & \cdots & \bar{f}_1(x_m^*) \\ \vdots & \ddots & & & \vdots \\ \bar{f}_i & \cdots & \bar{f}_i & \cdots & \bar{f}_i(x_m^*) \\ \vdots & & & \ddots & \vdots \\ \bar{f}_m(x_1^*) & \cdots & \bar{f}_m(x_i^*) & \cdots & \bar{f}_m(x_m^*) \end{bmatrix} \quad (1)$$

The ith row of the payoff matrix Φ includes the maximum and minimum values of the functions $f_i(x)$, representing their upper and lower limits. These values can be used to normalize the objective space, mainly by writing it in terms of different scales or units. The vector with the set of the individual minima $f^U = [f_1^*(x_1^*), \ldots, f_i^*(x_i^*), \ldots, f_m^*(x_m^*)]^T$ is called the *Utopia point*. The Utopia point, according to Vahidinasab and Jadid (2010), is a specific point, generally outside the feasible region, that corresponds to all objectives simultaneously being at their best possible values. In contrast, by constructing a vector with the maximum values of each objective function $f^N = \left[f_1^N, \ldots, f_i^N, \ldots, f_m^N\right]^T$, we obtain the *Nadir point*. This is the point where all objectives are simultaneously at their worst values. The Utopia and Nadir points make up the anchor points, which are obtained when the ith objective is minimized independently, while f_i^* represents the individual minima of the ith objective. All of the points mentioned above are illustrated for a bi-objective case in Fig. 1.

The normalization of the objective functions can be obtained by using the two following special sets:

$$\bar{f}(x) = \frac{f_i(x) - f_i^U}{f_i^N - f_i^U} \qquad i = 1, \ldots, m \tag{2}$$

This normalization leads to the normalized payoff matrix $\overline{\Phi}$.

An effective criterion to combine the mean and variance responses in dual response optimization is the mean square error (MSE). This approach has been used by such researchers as Köksoy (2006) and Vining and Myers (1990). The simultaneous optimization of mean and variance for multiple independent and uncorrelated responses subject only to the experimental region constraint (Cho & Park, 2005; Kazemzadeh et al., 2008; Kovach & Cho, 2009; Lee & Park, 2006; Paiva et al., 2012; Shin et al., 2011; Steenackers & Guillaume, 2008), can be seen in Eq. (3):

$$\begin{aligned} &\text{Minimize} \quad MSE = [\hat{\mu}(\mathbf{x}) - T]^2 + \sigma^2(\mathbf{x}) \\ &\text{Subject to} \quad \mathbf{x} \in \boldsymbol{\Omega} \end{aligned} \tag{3}$$

where T is the target for process mean $\mu(\mathbf{x})$. Thus, the expression $[\hat{\mu}(\mathbf{x}) - T]^2$ represents the mean deviation from the target, which would allow even greater reduction of variability in the process.

In certain cases, the mean and the variance can take different values due to the degree of importance assigned to each of them. To remedy this, the weighted MSE approach can be formulated as follows:

$$\begin{aligned} &\text{Minimize} \quad MSE_w = w_1[\hat{\mu}(\mathbf{x}) - T]^2 + w_2[\hat{\sigma}^2(\mathbf{x})] \\ &\text{Subject to} \quad \mathbf{x} \in \boldsymbol{\Omega} \end{aligned} \tag{4}$$

where the weights w_1 and w_2 are pre-specified positive constants (Kazemzadeh et al., 2008; Tang & Xu, 2002). By changing the weights, such that $w_1 + w_2 = 1$ and $w_1 > 0$, $w_2 > 0$, Tang and Xu (2002) showed that the multiple objective optimization generates a set of non-inferior solutions.

Based on combined arrays for a robust parameter optimization, Brito et al. (2014) implemented a dual response surface (DRS) method using the NBI algorithm and mean square error (MSE) functions for several characteristics with $f_i(x) = MSE_i(\mathbf{x})$, as proposed by Govindaluri and Cho (2007). Dealing with mean–variance optimization problems, their approach was capable of generating equally spaced Pareto Frontiers for bi-objective processes. The bi-dimensional NBI approach for MSE functions can be written as:

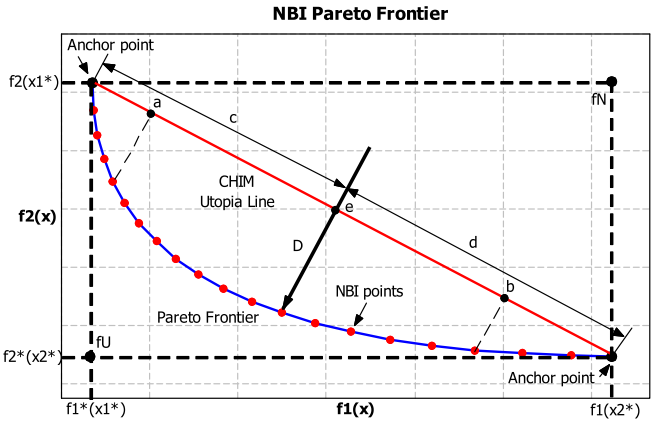

Fig. 1. NBI Pareto Frontier (Brito et al., 2014).

$$\begin{aligned} \text{Min } \bar{f}_1(\mathbf{x}) &= \left(\frac{MSE_i(\mathbf{x}) - MSE_i^I(\mathbf{x})}{MSE_i^{\max}(\mathbf{x}) - MSE_i^I(\mathbf{x})}\right) \\ \text{s.t.}: g_1(\mathbf{x}) &= \left(\frac{MSE_1(\mathbf{x}) - MSE_1^I(\mathbf{x})}{MSE_1^{\max}(\mathbf{x}) - MSE_1^I(\mathbf{x})}\right) - \left(\frac{MSE_2(\mathbf{x}) - MSE_2^I(\mathbf{x})}{MSE_2^{\max}(\mathbf{x}) - MSE_2^I(\mathbf{x})}\right) \\ &\quad + 2w - 1 = 0 \\ &\quad g_2(\mathbf{x}) = \mathbf{x}^{\mathbf{T}}\mathbf{x} \leqslant \rho^2 \\ &\quad 0 \leqslant w \leqslant 1 \end{aligned} \tag{5}$$

$$\text{with}: \quad MSE_i(\mathbf{x}) = (\hat{\mu}_i(\mathbf{x}) - T_i)^2 + \sigma_i^2(\mathbf{x}) \tag{6}$$

$$\hat{\mu}_i(\mathbf{x}) = E_z[y(\mathbf{x}, \mathbf{z})] \quad \text{and} \quad \sigma_i^2(\mathbf{x}) = \sigma_{z_i}^2 \left\{ \sum_{i=1}^{r} \left[\frac{\partial y(\mathbf{x}, \mathbf{z})}{\partial z_i}\right]^2 \right\} + \sigma^2$$

In Eq. (5), $MSE_i^I(\mathbf{x})$ is the utopia value used to optimize each $MSE_i(\mathbf{x})$, restricted only to the experimental region. The denominator $MSE_i^{\max}(\mathbf{x}) - MSE_i^I(\mathbf{x})$ is used to normalize the variability measures for the m Quality Characteristics – QCs (Govindaluri & Cho, 2007). It stands for the normalization of multiple responses, obtaining $MSE_i^{\max}(\mathbf{x})$ as the maximum value of the payoff matrix (matrix formed by all solutions observed in the individual optimizations).

However, most real problems are not limited to only two responses. Additionally, the correlation among responses can substantially influence the values of the $y(\mathbf{x}, \mathbf{z})$ regression coefficients (β_i), and this, according to Bratchell (1989), cannot be ignored. Such influence could impair the quality of DRS derived from $y(\mathbf{x}, \mathbf{z})$. The individual analysis of each response may lead to conflicting optima (Hair, Black, Babin, & Anderson, 2009; Yuan et al., 2008). One may deal with this correlation influence by using Principal Component Analysis (PCA).

3. Multivariate and multi-objective robust parameter optimization

PCA is a multivariate analysis technique used widely to reduce problem dimensionality and to extract information from original data through linear transformation (Xu & Lu, 2011). Johnson and Wichern (2007) described PCA as follows: Suppose that $f_1(x)$, $f_2(x), \ldots, f_p(x)$ are correlated functions written from a random vector $Y^T = [Y_1, Y_2, \ldots, Y_p]$. Accepting Σ as a variance–covariance matrix associated with this vector, then Σ can be factored into

pairs of eigenvalues–eigenvectors $(\lambda_i, e_i), \ldots \geqslant (\lambda_p, e_p)$ where $\lambda_1 \geqslant \lambda_2 \geqslant \cdots \geqslant \lambda_p \geqslant 0$ such that the ith linear combination is $PC_i = e_i^T Y = e_{1i}Y_1 + e_{2i}Y_2 + \cdots + e_{pi}Y_p$ with $i = 1, 2, \ldots, p$.

Paiva, Gomes, Peruchi, Leme, and Balestrassi (2014) proposed an alternative hybrid approach, combining response surface methodology (RSM) and PCA to optimize multiple correlated responses in a turning process. The constrained nonlinear programming problem written in terms of principal components could be expressed as shown in Eqs. (7) and (8).

$$\text{Minimize}: \ PC_1 = \beta_0 + \sum_{i=1}^{k}\beta_i x_i + \sum_{i=1}^{k}\beta_{ii}x_i^2 + \sum_{i<j}\sum\beta_{ij}x_i x_j \tag{7}$$

$$\text{Subject to}: \ x^{\mathrm{T}}x \leqslant \rho^2 \tag{8}$$

Optimal values can be obtained by locating the stationary point of the multivariate-fitted surface. The objective is to find the values of x's that optimize the multivariate objective function (PC_1), subject only to the constraint that defines the region of interest Ω. However, the first principal component alone may not explain the amount of variance–covariance structure of the original responses. Due to this drawback, Paiva et al. (2014) considered the eigenvalues of the correlation matrix as a set of weights used to combine the principal components into $WMI = \sum_{p=1}^{r}[\lambda_p(PC_p)]$. Therefore, the multivariate optimization problem can be written as:

$$\text{Miximize}: \ WMI = \beta_0 + \sum_{i=1}^{k}\beta_i x_i + \sum_{i=1}^{k}\beta_{ii}x_i^2 + \sum_{i<j}\sum\beta_{ij}x_i x_j \tag{9}$$

$$\text{Subject to}: \ x^{\mathrm{T}}x \leqslant \xi^2 \tag{10}$$

Extending the traditional mean square error (MSE) approach to the multivariate case, several authors (Gomes et al., 2013; Lopes et al., 2013; Paiva et al., 2014, 2012, 2009) have employed the multivariate mean square error (MMSE) method to optimize correlated multiple responses. In the original approach, Paiva et al. (2009) combined PCA and RSM to build MMSE functions to deal with multidimensional nominal-the-best problems. The MMSE formulation can be written as follows:

$$\begin{aligned}\text{Min } MMSE_T &= \left[\prod_{i=1}^{m}(MMSE_i|\lambda_i \geqslant 1)\right]^{\left(\frac{1}{m}\right)} \\ &= \left\{\prod_{i=1}^{m}\left[\left(PC_i - \zeta_{PC_i}\right)^2 + \lambda_i|\lambda_i \geqslant 1\right]\right\}^{\left(\frac{1}{m}\right)}, m \leqslant p \\ \text{S.t. } \mathbf{x}^{\mathrm{T}}\mathbf{x} &\leqslant \rho^2\end{aligned} \tag{11}$$

where

$$\zeta_{PC_i} = e_i^T\left[Z\left(Y_p|\zeta_{Y_p}\right)\right] = \sum_{i=1}^{p}\sum_{j=1}^{q}e_{ij}\left[Z\left(Y_p|\zeta_{Y_p}\right)\right] \quad i = 1, 2, \ldots, p; \quad j = 1, 2, \ldots, q \tag{12}$$

where m is the number of MMSE functions according to the significant principal components, PC_i is the fitted second-order polynomial, ζ_{PC_i} the target value of the ith principal component (that must keep a straightforward relation with the targets of the original data set), $\mathbf{x}^{\mathrm{T}}\mathbf{x} \leqslant \rho^2$ the experimental region constraint; e_i represents the eigenvector set associated with the ith principal component, and ζ_{Y_p} represents the target for each of the p original responses.

The model in Eq. (11) can be modified to reflect the degree of importance of the original responses. The alternative model was presented by Gomes et al. (2013):

$$\begin{aligned}&\text{Min } WMMSE_T = \sum_{i=1}^{m}\left[\frac{\upsilon_i}{\upsilon_T}.WMMSE_i\right] = \sum_{i=1}^{m}\left\{\frac{\upsilon_i}{\upsilon_T}.\left[\left(PC_i^* - \xi_{PC_i}\right)^2 + \lambda_i^*\right]\right\}.m \leqslant p \\ &\text{Subject to}: g_n(\mathbf{x}) \leqslant 0\end{aligned} \tag{13}$$

where $WMMSE_T$ is the Total Weighted Multivariate Mean Square Error, $WMMSE_i$ is the Weighted Multivariate Mean Square Error for the ith principal component, m the number of needed principal components, p the number of responses, υ_i the degree of explanation for the ith principal component, such that $\sum\upsilon_i = \upsilon_T$, PC_i^* the response surface function for the i$^{\text{th}}$ principal component obtained with the weighted responses, ζ_{PCi}^* the target for the ith principal component obtained with the weighted responses, λ_i^* the eigenvalue for the ith principal component obtained with the weighted responses, and $g_n(\mathbf{x}) \leqslant 0$ are the constraint equations.

When noise and the control variables are put together in a combined array, it is common to obtain a reduced value for the adjusted coefficient. When this happens, it is necessary to apply WLS to correct the fit of the model. Lopes et al. (2013) showed that by using the inverse of the multivariate uncertainty as a weighting matrix for principal component scores, it is possible to replace the original correlated dataset and achieve the desired level of R^2_{Adj}. Eq. 14 was used to identify the multivariable uncertainty. It was used in Eq. 15 for weighting the scores of the principal components by weighted least square (WLS):

$$\begin{aligned}u_m^2(PC) = &\left(\frac{e_1}{\sigma_{x_i}}\right)^2 u^2(x_i) + \left(\frac{e_2}{\sigma_{x_j}}\right)^2 u^2(x_j) + 2 \times \left(\frac{e_1}{\sigma_{x_i}}\right) \times \left(\frac{e_2}{\sigma_{x_j}}\right) \\ &\times u(x_i) \times u(x_j) \times r(x_i, x_j)\end{aligned} \tag{14}$$

$$W_{(PC)} = \left(\frac{1}{u_m^2(PC)}\right) \tag{15}$$

Taguchi (1986) proposed a set of techniques to identify the values of $\boldsymbol{x}$ to achieve a robust performance. The control parameters $\boldsymbol{x}$ were varied according to an orthogonal array (“control” or “inner” array). In each setting of the control parameters, the effects of noise variables were evaluated by varying them systematically using a “noise” or “outer” array. The main objective was to identify the appropriate settings of the control parameter at which the system's performance remains robust against uncontrollable variations in $\boldsymbol{z}$ (Shahriari, Haji, & Eslamipoor, 2014). Montgomery (2009) found that these interactions could not be estimated since the means and variances were in a crossed array structure, calculated over the same levels of noise variables. To circumvent this situation, Vining and Myers (1990) proposed alternatives to Taguchi's model. They combined control and noise factors in a single array, so that noise and control interactions could be estimated. The general response surface model involving control and noise variables, organized in a combined array, may be written as:

$$\begin{aligned}y(\mathbf{x}, \mathbf{z}) = &\beta_0 + \sum_{i=1}^{k}\beta_i x_i + \sum_{i=1}^{k}\beta_{ii}x_i^2 + \sum_{i<j}\sum\beta_{ij}x_i x_j + \sum_{i=1}^{r}\gamma_i z_i \\ &+ \sum_{i=1}^{k}\sum_{j=1}^{r}\delta_{ij}x_i z_j + \varepsilon\end{aligned} \tag{16}$$

where k and r are the number of control and noise variables.

Assuming that noise variables and random error are not correlated and that the variables are independent with zero mean and variance (σ_z^2), Montgomery (2009) showed that the models for the mean and variance can be written as:

$$E_z[y(\mathbf{x}, \mathbf{z})] = f(\mathbf{x}) \tag{17}$$

$$V_z[y(\mathbf{x}, \mathbf{z})] = \sigma_{z_i}^2\left\{\sum_{i=1}^{r}\left[\frac{\partial y(\mathbf{x}, \mathbf{z})}{\partial z_i}\right]^2\right\} + \sigma^2 \tag{18}$$

In a multivariate context, Paiva et al. (2012) integrated MMSE functions to RPD designs based on crossed arrays. Their MRPD approach consisted of calculating MSE functions for each run in a

crossed array. After that, scores of principal components are obtained from MSEs, and the MMSE (MRPD) model is applied according to Eqs. (11) and (12). Conjoining PCA and RPD based on combined array, Paiva et al. (2014) proposed a optimization method to minimize the noise variables' effects on multiple correlated QCs. In their approach, the weighted sum of multivariate mean square error functions for the mean and variance blocks have been implemented according to Eqs. (19) and (20):

$$\text{Min } F(\mathbf{x}) = \left\{ \prod_{i=1}^{m} \left[\begin{array}{c} \omega \cdot \left(E_z\left[P_c(\mathbf{x},\mathbf{z})_i\right] - \zeta_{PCz_i}\right)^2 + \\ (1-\omega)\cdot\left[\sigma_z^2 \cdot \sum_{j=1}^{r}\left(\frac{\partial P_c(\mathbf{x},\mathbf{z})_i}{\partial z_j}\right)^2 + \sigma^2\right] \end{array} \right]^{\phi_i} \middle| \sum_{i=1}^{m-r}\phi_i \geqslant \xi \right\}^{\left(\frac{1}{\sum_{i=1}^{m-r}\phi_i}\right)} \quad (19)$$

$$\text{s.t.: } \mathbf{x}^T\mathbf{x} \leqslant \rho^2$$

$$\text{with: } \zeta_{PCz_i} = e_{1i}\left[Z\left(Y_1|\zeta_{Y_1}\right)\right] + e_{2i}\left[Z\left(Y_2|\zeta_{Y_2}\right)\right] + \cdots + e_{pi}\left[Z\left(Y_p|\zeta_{Y_p}\right)\right] \quad (20)$$

$$P_c(\mathbf{x},\mathbf{z})_i = \left(\beta_0 + \sum_{i=1}^{k}\beta_i x_i + \sum_{i=1}^{k}\beta_{ii}x_i^2 + \sum_{i<j}\sum\beta_{ij}x_i x_j + \sum_{i=1}^{k}\gamma_i z_i + \sum_{i=1}^{k}\sum_{j=1}^{r}\delta_{ij}x_i z_j + \varepsilon\right)_i$$

$$i = 1,2,\ldots,m$$

$$\mathbf{x} = [x_1, x_2, \ldots, x_k]$$

$$\mathbf{z} = [z_1, z_2, \ldots, z_r]$$

The value of ζ_{Y_p} corresponds to a single objective optimization obtained as $\zeta_{Y_p} = Min_{\mathbf{x}\in\Omega}[\hat{y}_i(\mathbf{x})]$ and Z represents the standardized value of the ith response considering the target ζ_{Y_p}, such that $Z(Y_p|\zeta_{Yp}) = \left[(\zeta_{Yp}) - \mu_{Yp}\right] \times (\sigma_{Yp})^{-1}$. Furthermore, the term ϕ_i is an exponent that stands for the relative importance of each principal component.

4. NBI coupled with PCA for combined arrays

Consider now the use of the NBI method combined with the PCA optimization routine. First, it is necessary to establish two functions: $f_{(\mu)}(\mathbf{x})$, which represents the block of the correlated mean responses, and $f_{(\sigma^2)}(\mathbf{x})$, which represents the block of variance responses, as such:

$$f_{(\mu)}(\mathbf{x}) = \left[\sum_{i=1}^{p}\lambda_p\left(\frac{PC_{(\mu)_i} - \zeta_{PC(\mu)_i}}{\zeta_{PC(\mu)_i}}\right)^2\right] \quad (\lambda_p \geqslant 1) \cup \left(\frac{\lambda_p}{\sum\lambda_p} \geqslant \xi\right)$$
$$p = 1,2,\ldots,P \quad (21)$$

$$f_{(\sigma^2)}(\mathbf{x}) = \left[\sum_{i=1}^{p}\lambda_p\left(\frac{PC_{(\sigma^2)_i} - \zeta_{PC(\sigma^2)_i}}{\zeta_{PC(\sigma^2)_i}}\right)^2\right] \quad (\lambda_p \geqslant 1) \cup \left(\frac{\lambda_p}{\sum\lambda_p} \geqslant \xi\right)$$
$$p = 1,2,\ldots,P \quad (22)$$

Considering the payoff matrix established for $f_{(\mu)}(\mathbf{x})$ and $f_{(\sigma^2)}(\mathbf{x})$, we obtain the following normalized performance measures:

$$\bar{f}_{(\mu)}(x) = \frac{f_{(\mu)}(x) - f^U_{(\mu)}}{f^N_{(\mu)} - f^U_{(\mu)}} = \frac{f_{(\mu)}(x) - f^I_{(\mu)}}{f^{MAX}_{(\mu)} - f^I_{(\mu)}} \quad (23)$$

$$\bar{f}_{(\sigma^2)}(x) = \frac{f_{(\sigma^2)}(x) - f^U_{(\sigma^2)}}{f^N_{(\sigma^2)} - f^U_{(\sigma^2)}} = \frac{f_{(\sigma^2)}(x) - f^I_{(\sigma^2)}}{f^{MAX}_{(\sigma^2)} - f^I_{(\sigma^2)}} \quad (24)$$

Using the original NBI formulation, the optimization RPD-MNBI approach can be written as:

$$\text{Min } \bar{f}_{(\mu)}(\mathbf{x}) = \left[\frac{f_{(\mu)}(\mathbf{x}) - f^I_{(\mu)}}{f^{MAX}_{(\mu)} - f^I_{(\mu)}}\right]$$

$$\text{s.t.: } \bar{g}_{1_{(\mu,\sigma^2)}}(\mathbf{x}) = \left[\frac{f_{(\mu)}(\mathbf{x}) - f^I_{(\mu)}}{f^{MAX}_{(\mu)} - f^I_{(\mu)}}\right] - \left[\frac{f_{(\sigma^2)}(\mathbf{x}) - f^I_{(\sigma^2)}}{f^{MAX}_{(\sigma^2)} - f^I_{(\sigma^2)}}\right] + 2w_i - 1 = 0 \quad (25)$$

$$g_2(\mathbf{x}) = \mathbf{x}^T\mathbf{x} \leqslant \rho^2$$

$$0 \leqslant w_i \leqslant 1$$

$$PC(\mathbf{x})_i = \left(\beta_0 + \sum_{i=1}^{k}\beta_i x_i + \sum_{i=1}^{k}\beta_{ii}x_i^2 + \sum_{i<j}\sum\beta_{ij}x_i x_j + \varepsilon\right)_i \quad (26)$$

$$i = 1,2,\ldots,p; \quad j = 1,2,\ldots,q$$

To illustrate the RPD-MNBI procedure, Fig. 2 shows the overall structure, consisting of nine steps. In **Step 1**, an adequate combined array is defined as the experimental design, including as many control and noise variables as desired. The experiments are run in a random order and the responses are stored. In **Step 2**, the results from Step 1 are used to identify the correlation between the responses, and PCA is performed. Using the correlation matrix, PC scores are extracted from the original responses and they are stored with the respective eigenvalues and eigenvectors. In **Step 3**, the *OLS* algorithm is used and the results are analyzed. In PCA, the number of PCs is chosen to explain at least 80% of the model variance. The obtained R^2_{Adj} is important for the models. If the R^2_{Adj} is inadequate, the approach used by Lopes et al. (2013) and defined by Eq. (14) is used for PCA, while for the original response, WLS is used (as described in Step 4). In **Step 4**, the WLS method is applied to the original responses using as weights the inverse of the quadratic residuals. For PCA, the inverse of multivariate uncertainty generated by Eq. (15) is used as the weight. In **Step 5**, the equations for the mean and variance of $y(\mathbf{x},\mathbf{z})_i$ and $P_c(\mathbf{x},\mathbf{z})_i$ are computed using Eqs. (17) and (18). In **Step 6**, the response targets $\left(\zeta_{Y_p}\right)$ are obtained using the individual constrained minimization of each response surface, i.e. $\zeta_{Y_p} = Min_{\mathbf{x}\in\Omega}[\hat{y}_i(\mathbf{x})]$ and the original targets $\left(\zeta_{Y_p}\right)$ are transformed in PC-targets using the identity $\zeta_{PC_i} = \sum_{i=1}^{p}\sum_{j=1}^{q}e_{ij}\left[Z\left(Y_p|\zeta_{Y_p}\right)\right]$. In **Step 7**, the desired values for $\boldsymbol{\omega}_\mu$ and $\boldsymbol{\omega}_{\sigma^2}$ (mean and variance weights) are chosen, generally using the range [0; 1], and the value of the percentage of explanation for $PC_i(\phi_i)$ is observed. This value is needed only if the practitioner needs more than one principal component. In **Step 8**, the payoff matrix calculation is performed using mean, variance, and targets to build each MSE function for individual responses or for each PC. After that, the individual optimization (Eq. (1)) of each PC function is computed as: $Min_{x\in\Omega}\left[\left(PC_{(\mu)_i} - \zeta_{PC(\mu)_i}\right)/\zeta_{PC(\mu)_i}\right]^2 + \sigma^2$. Then the scalarization of PC_1 for a bivariate case is computed according to Eqs. (23) and (24). In **Step 9**, using the generalized reduced gradient (GRG) algorithm, the minimum value of the MSE or PC (Fi)(x)—computed in Step 8—is obtained using as constraints the experimental region, non-negative variances, or some other constraint $gi(x)$ desired by the practitioner. Then a uniform spread of the Pareto Frontier is created from these results.

5. Experiment, results and discussion

This section presents a numerical illustration of our model and checks its acceptability. It also compares the results from the following methods: Weighted Sum, NBI-MSE, and RPD-MNBI.

5.1. Experiment description

To achieve this paper's aims, a set of 82 experiments, provided by Brito et al. (2014), were carried out in a finishing end milling operation of AISI 1045 steel. The tool used was a positive end mill, code R390–025A25-11 M with a 25 mm diameter, an entering angle of $\chi_r = 90°$, and a medium step with 3 inserts. Three rectangular inserts were used with edge lengths of 11 mm each, code R390-11T308M-PM GC 1025 (Sandvik, 2010). The tool material used was cemented carbide ISO P10 coated with TiCN and TiN via the PVD process. The coating hardness was approximately 3000 HV3 and the substrate hardness 1650 HV3, with a grain size smaller than 1 μm.

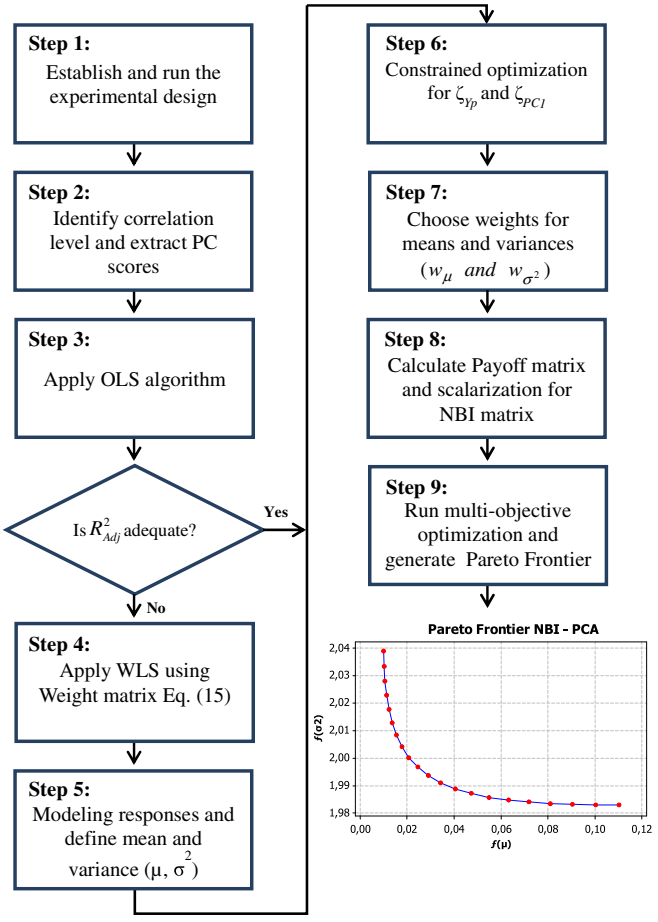

Fig. 2. Overview of the proposed procedure.

The work piece material was AISI 1045 steel with a hardness of approximately 180 HB. The work piece dimensions were rectangular blocks with square sections of 100 × 100 mm and lengths of 300 mm. All the milling experiments were carried out in a FADAL vertical machining center, model VMC 15, with a maximum spindle rotation of 7500 RPM and 15 kW of power in the main motor. The tool overhang was 60 mm. The cutting fluid used in the experiments was synthetic oil Quimatic MEII. Following the experimental sequence for a combined array suggested by Montgomery (2009), a CCD for $k = 7$ variables ($x_1, x_2, x_3, x_4, z_1, z_2$ and z_3) with 10 center points were created, also deleting the axial points related to the noise variables. The levels for control and noise factors are described in Tables 1 and 2, respectively (Lopes, Brito, Paiva, Peruchi, & Balestrassi, in press) here reproduced.

The different noise conditions furnished by a combination of factors and levels described in Table 2 express, in some sense, the possible variation that can occur during the end milling operation, such as the tool flank wear (z_1), the variations in cutting fluid concentration (z_2), and the variation of cutting fluid flow rate (z_3). The surface roughness values are expected to suffer some kind of variation due to the action of the combined noise factors. Therefore, RPD's main objective is to determine the setup of control parameters capable of achieving a reduced surface roughness with minimal variance, mitigating the influence of noise factors on the process performance.

Measurements of the tool flank wear $(VB_{max})(z_1)$ were captured with an optical microscope (magnification 45X) with images acquired by a coupled digital camera. The criteria adopted as the end of tool life was a flank wear of approximately $VB_{max} = 0.30$ mm.

The responses measured in the end milling process were R_a (the arithmetic average surface roughness) and R_t (the maximum roughness height - distance from highest peak to lowest valley). These QCs were assessed using a Mitutoyo portable roughness meter, model Surftest SJ 201, with a cut-off length of 0.25 mm. This procedure resulted in 82 experiments, described in Lopes et al. (in press). The two surface roughness metrics were measured three times at each of three positions on the work piece, computed after determining the mean of the nine measurements.

5.2. Results from the Weighted Sums and NBI-MSE methods

The Pearson's correlation (Step 2) of R_a and R_t was 0.965 with a P-value = 0.000, representing a strong level of correlation with statistical significance. The OLS algorithm (Step 4) produced R^2_{Adj} of R_a of 70.08% and 71.22% for R_t. Both results can be considered unacceptable for the model. Thus, applying the WLS method, using as weights the inverse of the quadratic residual (Step 5), the response surfaces with R^2_{Adj} for $R_a = 99.9\%$ and $R_t = 99.1\%$ were obtained and given by the following equations:

$$\begin{aligned} R_a(x,z) = {} & 0.689 + 0.898x_1 + 0.041\,x_2 - 0.066\,x_3 - 0.004\,x_4 \\ & + 0.102\,z_{1^1} + 0.002z_2 + 0.005\,z_3 + 0.493\,x_1^2 \\ & + 0.096\,x_2^2 + 0.010x_3^2 + 0.064\,x_4^2 + 0.074\,x_1x_2 \\ & - 0.088\,x_1x_3 + 0.030\,x_1x_4 + 0.048\,x_1z_1 \\ & - 0.086\,x_1z_2 + 0.042\,x_1z_3 - 0.039\,x_2x_3 \\ & + 0.018x_2x_4 + 0.013\,x2z1 - 0.073\,x_2z_2 \\ & - 0.012\,x_2z_3 + 0.043\,x_3x_4 + 0.020\,x_3z_1 \\ & - 0.034\,x_3z_2 - 0.041\,x_3z_3 - 0.052\,x_4z_1 \\ & - 0.013\,x_4z_2 - 0.025\,x_4z_3 \end{aligned} \quad (27)$$

$$\begin{aligned} R_t(x,z) = {} & 4.72 + 3.17\,x_1 + 0.251\,x_2 - 0.261\,x_3 + 0.046\,x_4 \\ & + 0.877\,z_1 + 0.040\,z_2 - 0.049\,z_3 + 1.04\,x_1^2 \\ & + 0.176\,x_2^2 + 0.000\,x_3^2 + 0.173\,x_{34}^2 + 0.498\,x_1x_2 \\ & - 0.225\,x_1x_3 + 0.233\,x_1x_4 + 0.310\,x_1z_1 \\ & - 0.291\,x_1z_2 + 0.188\,x_1z_3 - 0.0205\,x_2x_3 \\ & + 0.164\,x_2x_4 - 0.087\,x_2z_1 - 0.210\,x_2z_2 \\ & - 0.127\,x_2z_3 + 0.181\,x_3x_4 + 0.128\,x_3z_1 \\ & - 0.109\,x_3z_2 + 0.042\,x_3z_3 - 0.158x_4z_1 \\ & - 0.016\,x_4z_2 + 0.157\,x_4z_3 \end{aligned} \quad (28)$$

Table 1
Control factors and respective levels.

Parameters	Unit	Symbol	Levels				
			−2.828	−1.000	0.000	1.000	2.828
Feed rate, x_1	mm/tooth	*fz*	0.01	0.10	0.15	0.20	0.29
Axial depth of cut, x_2	mm	*ap*	0.064	0.750	1.125	1.500	2.186
Cutting speed, x_3	m/min	*Vc*	254	300	325	350	396
Radial depth of cut, x_4	mm	*ae*	12.26	15.00	16.50	18.00	20.74

Table 2
Noise factors and respective levels.

Noise factors	Unit	Symbol	Levels		
			−1	0	+1
Tool flank wear	Mm	Z_1	0.00	0.15	0.30
Cutting fluid concentration	%	Z_2	5	10	15
Cutting fluid flow rate	l/min	Z_3	0	10	20

Table 3
PCA: R_a and R_t.

Eigenvalue	1.9651	0.0349
Proportion	0.9830	0.0170
Cumulative	0.9830	1.0000
Eigenvectors	PC_1	PC_2
R_a	0.7070	0.7070
R_t	0.7070	−0.7070

Table 4
Pay off matrix.

$PC(\mu)_1$	$PC_{(\sigma 2)_1}$
0.01007	0.11021
2.03894	1.98296

Following Steps 6, 7, and 8, the mean and variance are computed using the combined array written in terms of only control variables, although the noise factors were used during the experimentation. To perform the payoff matrix calculation for a bi-objective case, Eq. (29) is used:

$$\Phi = \begin{bmatrix} MSE_1^I(\mathbf{x}) & MSE_1^{\max}(\mathbf{x}) \\ MSE_2^{\max}(\mathbf{x}) & MSE_2^1(\mathbf{x}) \end{bmatrix} \tag{29}$$

In Step 12, using the values of the Payoff matrix, the scalarization of the MSE function is obtained. For the bivariate case, Eq. (30) is used.

$$\bar{f}(x) = \frac{f_i(x) - f_i^U}{f_i^N - f_i^U} \Rightarrow \left\{ \begin{array}{l} \bar{f}_1(x) = \overline{MSE_1}(x) = \frac{MSE_1(x) - MSE_1^I}{MSE_1^{Max} - MSE_1^I} \\ \bar{f}_2(x) = \overline{MSE_2}(x) = \frac{MSE_2(x) - MSE_2^I}{MSE_2^{Max} - MSE_2^I} \end{array} \right\} \tag{30}$$

The generalized reduced gradient (GRG) algorithm is used to minimize the MSE. However, given that the variance equation takes the noise effect into account, the adjustment of the control factors leads to the minimization of the process variability, guaranteeing the robustness of the end milling process.

5.3. Results of RPD-MNBI for combined array

Results showed that the two original responses, R_a and R_t, were strongly dependent (0.965 with P-value = 0.000). The PC scores were extracted and the OLS algorithm was applied. It can be observed that the first principal component, shown in Table 3, explains about 98.30% of variance–covariance structure established between R_a and R_t and that the R^2_{Adj} value is 71.63%.

The approach used by Lopes et al. (2013) and shown in Eq. (14) was used, and the WLS method was applied using as a weighted matrix the inverse of the multivariate uncertainty for the PC calculated by Eq. (15). As a result, R^2_{Adj} = 96.90% and the respective $PC_{1\,(RaRt)}$ equations can be written as:

$$\begin{aligned} \mu[\mathrm{PC}_{(x,z)}] = & -0.655 + 1.344\,x_1 + 0.102\,x_2 - 0.119\,x_3 \\ & + 0.0175\,x_4 + 0.265 z_1 + 0.0084\,z_2 - 0.0100\,z_3 \\ & + 0.623\,x_1x_1 + 0.106\,x_2x_2 + 0.0181\,x_3x_3 \\ & + 0.0843\,x_4x_4 + 0.165\,x_1x_2 - 0.122\,x_1x_3 \\ & + 0.102\,x_1x_4 + 0.133\,x_1z_1 - 0.138\,x_1z_2 \\ & + 0.0702\,x_1z_3 - 0.0394\,x_2x_3 + 0.0588\,x_2x_4 \\ & + 0.0030\,x_2z_1 - 0.113\,x_2z_2 - 0.0495\,x_2z_3 \\ & + 0.0678\,x_3x_4 + 0.0392\,x_3z_1 - 0.0476\,x_3z_2 \\ & - 0.0108\,x_3z_3 - 0.0609\,x_4z_1 - 0.0365\,x_4z_2 \\ & + 0.0271\,x_4z_3 \end{aligned} \tag{31}$$

and

$$\begin{aligned} \sigma^2[\mathrm{PC}_{(x,z)}] = & (0.2651 + 0.1333\,x_1 + 0.0030\,x_2 + 0.0392\,x_3 - 0.0609\,x_4)^2 \\ & + (0.0084 - 0.1377\,x_1 - 0.1128\,x_2 - 0.0476\,x_3 - 0.0365\,x_4)^2 \\ & + (-0.0100 + 0.0702\,x_1 - 0.0495\,x_2 - 0.0108\,x_3 + 0.0271\,x_4)^2 \end{aligned} \tag{32}$$

Table 5
Optimization results for RPD-MNBI.

Weights		Coded parameters				Responses				$f_{(\mu)}$	$f_{(\sigma 2)}$
W_1	W_2	x_1	x_2	x_3	x_4	R_a	R_t	*Var Ra*	*Var Rt*		
1.00	0.00	−1.239	−0.008	−1.263	0.933	0.262	2.076	0.920	1.335	0.010	2.039
0.95	0.05	−1.230	0.056	−1.241	0.972	0.264	2.074	0.919	1.312	0.010	2.033
0.90	0.10	−1.220	0.119	−1.214	1.012	0.267	2.078	0.917	1.290	0.011	2.028
0.85	0.15	−1.209	0.183	−1.182	1.053	0.271	2.088	0.915	1.269	0.011	2.023
0.80	0.20	−1.197	0.245	−1.144	1.095	0.277	2.105	0.914	1.247	0.012	2.018
0.75	0.25	−1.183	0.305	−1.100	1.140	0.285	2.130	0.913	1.225	0.014	2.013
0.70	0.30	−1.167	0.361	−1.048	1.188	0.294	2.165	0.911	1.205	0.015	2.008
0.65	0.35	−1.148	0.409	−0.984	1.236	0.303	2.211	0.910	1.185	0.018	2.004
0.60	0.40	−1.124	0.442	−0.861	1.256	0.313	2.278	0.909	1.168	0.021	2.000
0.55	0.45	−1.098	0.469	−0.766	1.308	0.324	2.349	0.908	1.151	0.025	1.997
0.50	0.50	−1.071	0.486	−0.698	1.381	0.337	2.425	0.907	1.135	0.029	1.994
0.45	0.55	−1.043	0.495	−0.651	1.466	0.351	2.505	0.907	1.121	0.034	1.991
0.40	0.60	−1.013	0.492	−0.594	1.542	0.365	2.593	0.907	1.111	0.041	1.989
0.35	0.65	−0.978	0.475	−0.515	1.598	0.378	2.692	0.907	1.105	0.047	1.987
0.30	0.70	−0.939	0.453	−0.451	1.646	0.391	2.794	0.907	1.102	0.055	1.986
0.25	0.75	−0.898	0.431	−0.410	1.685	0.402	2.895	0.906	1.101	0.063	1.985
0.20	0.80	−0.856	0.412	−0.393	1.716	0.413	2.994	0.906	1.102	0.072	1.984
0.15	0.85	−0.814	0.398	−0.397	1.738	0.424	3.089	0.906	1.103	0.081	1.983
0.10	0.90	−0.774	0.389	−0.415	1.754	0.434	3.178	0.905	1.105	0.091	1.983
0.05	0.95	−0.736	0.382	−0.442	1.766	0.444	3.262	0.905	1.106	0.100	1.983
0.00	1.00	−0.701	0.378	−0.473	1.772	0.454	3.340	0.904	1.108	0.110	1.983

Correlation = 0.9916

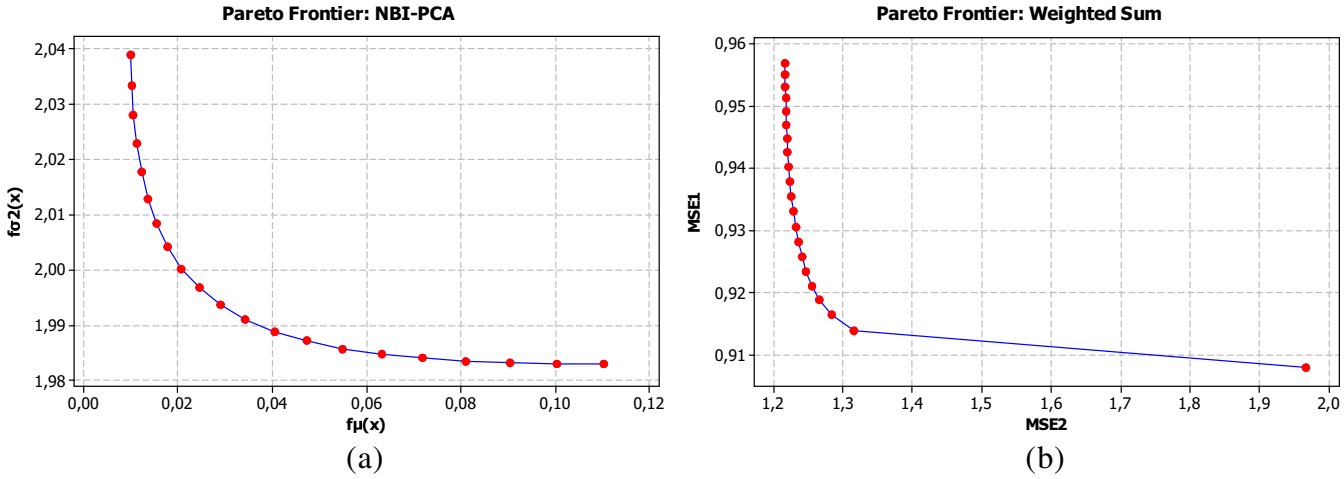

Fig. 3. Pareto Frontier with NBI-PCA and WS methods.

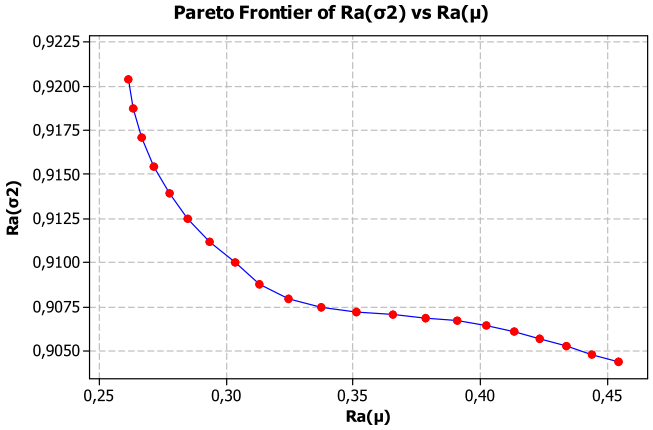

Fig. 4. Pareto Frontier for R_a.

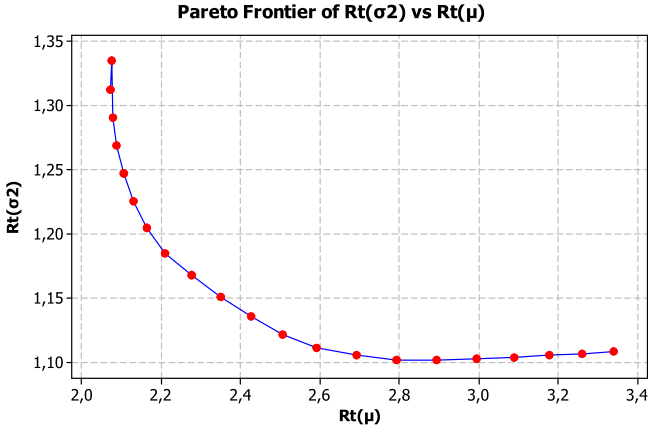

Fig. 5. Pareto Frontier for R_t.

Now, using Eqs. (21) and (22), we obtain $f_{(\mu)}(\mathbf{x}) = 0.029$ and $f_{(\sigma^2)}(\mathbf{x}) = 1.994$ and their values can be used in the NBI method with PCA optimization. The next step is the computation of the payoff matrix based on Eqs. (21) and (22). The payoff matrix is shown in Table 4.

The optimization approach through RPD-MNBI, written as Eq. (25), produced roughness values for R_a and R_t and also measures

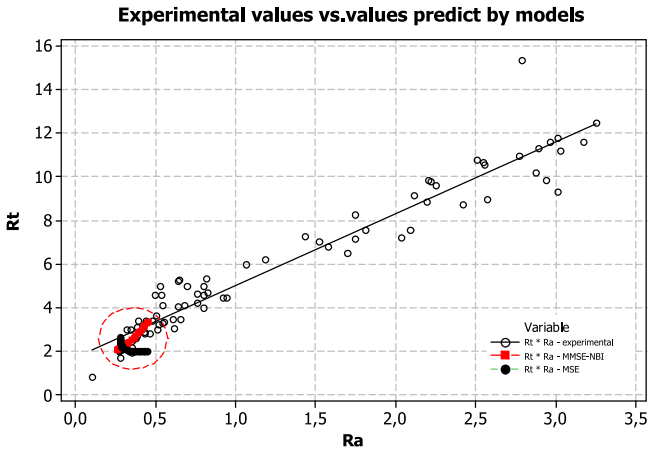

Fig. 6. Experimental values vs. values predicted by RPD-MNBI and MSE methods.

for $f_{(\mu)}(\mathbf{x})$ and $f_{(\sigma^2)}(\mathbf{x})$, that are given in Table 5. Notice that the correlation that existed in the original response remains present for roughness values generated by the optimization model. Thus, we can conclude that the correlation present in the original responses are passed on to the scores of principal components, which in turn are transferred to the responses generated by the optimization model.

As a result of these transfers, a Pareto optimal surface, given in Fig. 3(a), was generated as expected and can be compared with the frontier generated by the method of weighted sums in Fig. 3(b).

The Pareto Frontiers generated for the mean versus variance of R_a and R_t are given in Figs. 4 and 5.

In Fig. 6, three sets of data are displayed. The experimental values are represented by white circles, the values predicted by the MSE model are in black bullets, and the optimum values predicted by the RPD-MNBI model are in red squares. Notice that the greatest concentration is located at the bottom of the graph, due to the equation that minimized the roughness values.

Focusing on the lower end of the graph, as shown in Fig. 7, notice that the values predicted by the MSE model deviate from the experimental data set and the optimum values predicted by RPD-MNBI model.

The mean square error (MSE) was the method applied to generate the optimum points given by the set of black bullets in the orthogonal observed in Fig. 8. This optimization produced a

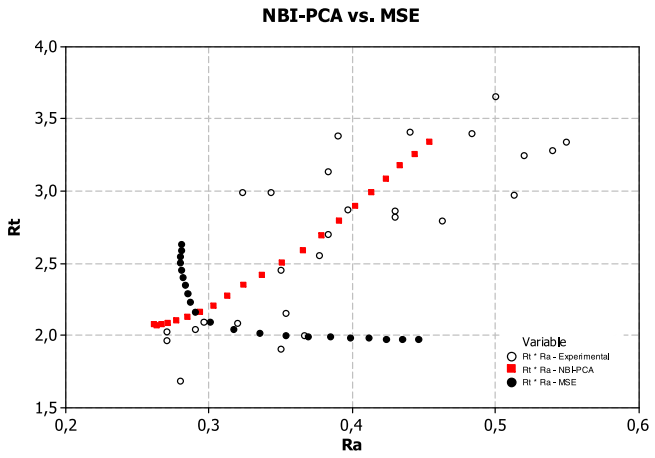

Fig. 7. Zooming in on the optimal points.

negative correlation (−0.8023, see Table 6) for R_a and R_t roughness, whereas, RPD-MNBI method generated optimum points given in red squares which preserved a positive correlation (0.9916), shown above in Table 5.

Govindaluri and Cho (2007) applied the MSE method in a robust design modeling with correlated QCs. They reported that these models either considered independent QCs or investigated the RD optimization for a single QC. Govindaluri and Cho (2007) further showed that these models had not clearly captured statistical correlations among QCs.

In conclusion, the evidence cited above must explain why the MSE model independently calculated the values for R_a and R_t and as a result generated a negative correlation.

5.4. Validation runs

In robust design optimization the idea is to discover a configuration of control factors that are insensitive to the actions of the uncontrollable ones. But before performing the validation runs, it is necessary to define the size of the experiment. Initially, power and sample size sensitivities were performed to guarantee enough certainty in detecting differences of magnitude 0.2 for R_a and 1.8 for R_t. Fig. 8(a), (b), and (c) shows the power curves for R_a based on the variance with $w = 0.1$, $w = 0.5$ and $w = 0.9$. The power curves for R_t was performed on the same basis.

Thus, the power curve with $w = 0.1$, $w = 0.5$, and $w = 0.9$ indicate the need for 4, 5, and 10 samples, with power over 82%. As a result, 27 samples were chosen.

To test this claim with the process under study, L9 Taguchi design was used to assess the behavior of the optimum setup in a range of scenarios formed by the noise factors. If the setup is to be robust, the noise factors will be statistically insignificant when the L9 analysis is performed. The validation runs began with the choosing of 3 from 21 points on the Pareto Frontier. The optimal condition associated with the weights $w = 0.10$, $w = 0.50$, and $w = 0.90$ were chosen. At these levels of importance, the optimum vectors (in coded units) were $\mathbf{X}^*_{w=0.10} = [-0.774 \;\; 0.389 - 0.415 \;\; 1.754]$, $\mathbf{X}^*_{w=0.50} = [-1.071 \;\; 0.486 - 0.698 \;\; 1.381]$ and $\mathbf{X}^*_{w=0.90} = [-1.220 \;\; 0.119 - 1.214 \;\; 1.012]$. Keeping these setups fixed along

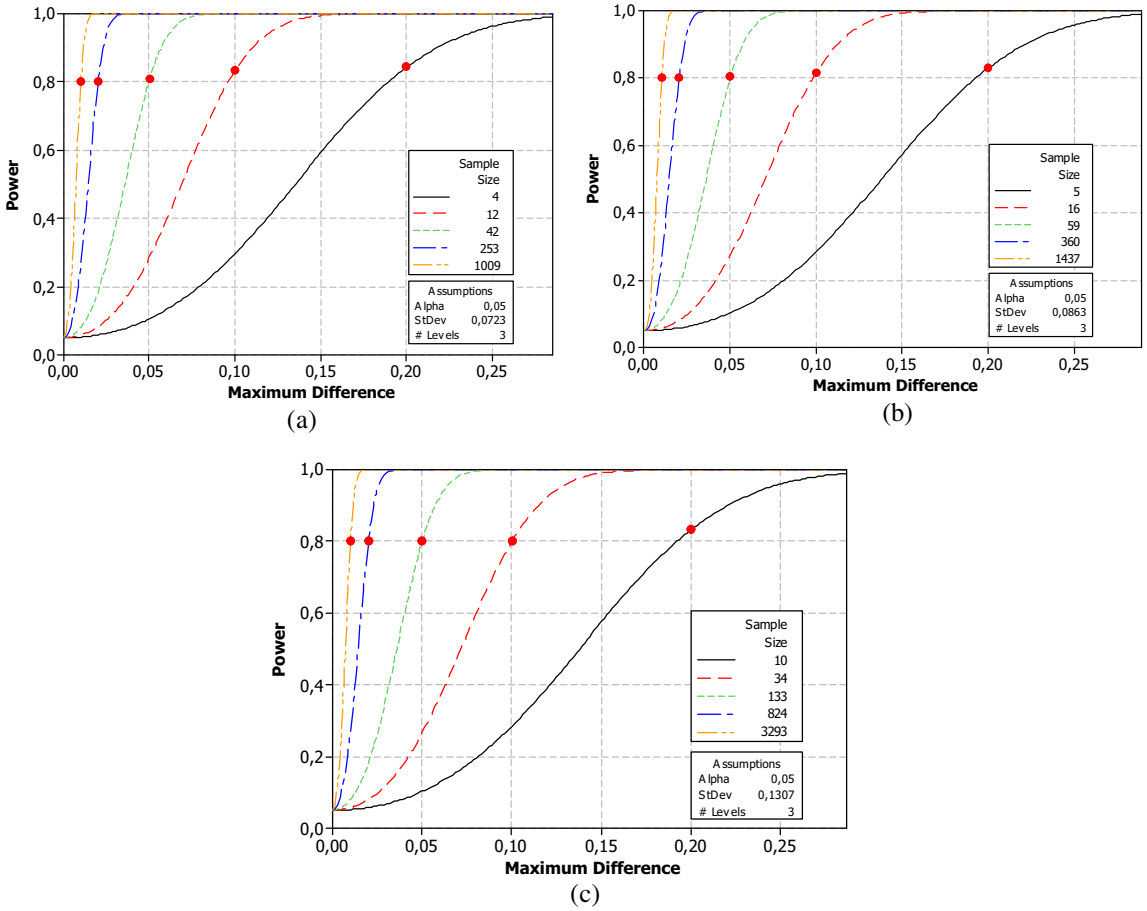

Fig. 8. Power curve with $w = 0.1$(a), $w = 0.5$ (b) and $w = 0.9$ (c).

Table 6
Optimization by MSE model.

Weights		NBI									
W_1	W_2	x_1	x_2	x_3	x_4	R_a	R_t	$\sigma^2 R_a$	$\sigma^2 R_t$	MSE_1	MSE_2
0.00	1.00	−1.4502	0.8551	−0.3471	1.0223	0.4461	1.9773	0.9101	1.1843	0.9568	1.2173
0.05	0.95	−1.4344	0.8423	−0.4079	1.0328	0.4352	1.9791	0.9099	1.1840	0.9519	1.2177
0.10	0.90	−1.4180	0.8263	−0.4716	1.0413	0.4236	1.9811	0.9097	1.1844	0.9471	1.2188
0.15	0.85	−1.4007	0.8070	−0.5384	1.0473	0.4114	1.9835	0.9095	1.1855	0.9424	1.2209
0.20	0.80	−1.3824	0.7839	−0.6088	1.0506	0.3984	1.9867	0.9093	1.1875	0.9377	1.2241
0.25	0.75	−1.3626	0.7570	−0.6837	1.0502	0.3845	1.9910	0.9092	1.1905	0.9331	1.2287
0.30	0.70	−1.3407	0.7256	−0.7643	1.0450	0.3695	1.9972	0.9092	1.1946	0.9286	1.2353
0.35	0.65	−1.3156	0.6893	−0.8521	1.0334	0.3532	2.0066	0.9092	1.2001	0.9243	1.2447
0.40	0.60	−1.2857	0.6485	−0.9488	1.0130	0.3355	2.0221	0.9092	1.2071	0.9204	1.2585
0.45	0.55	−1.2480	0.6066	−1.0543	0.9813	0.3170	2.0497	0.9093	1.2148	0.9168	1.2795
0.50	0.50	−1.1993	0.5742	−1.1591	0.9425	0.3006	2.0985	0.9091	1.2202	0.9141	1.3121
0.55	0.45	−1.1463	0.5525	−1.2240	0.9090	0.2902	2.1677	0.9086	1.2205	0.9122	1.3592
0.60	0.40	−1.1151	0.5350	−1.1064	0.8337	0.2872	2.2349	0.9077	1.2221	0.9110	1.4152
0.65	0.35	−1.0843	0.5162	−1.0062	0.7777	0.2848	2.2967	0.9071	1.2248	0.9101	1.4761
0.70	0.30	−1.0546	0.4974	−0.9201	0.7333	0.2829	2.3539	0.9066	1.2285	0.9094	1.5404
0.75	0.25	−1.0259	0.4781	−0.8467	0.6977	0.2816	2.4073	0.9062	1.2331	0.9089	1.6074
0.80	0.20	−0.9984	0.4580	−0.7842	0.6690	0.2807	2.4575	0.9059	1.2382	0.9085	1.6766
0.85	0.15	−0.9719	0.4374	−0.7306	0.6456	0.2802	2.5051	0.9057	1.2438	0.9082	1.7475
0.90	0.10	−0.9465	0.4162	−0.6842	0.6260	0.2801	2.5505	0.9055	1.2497	0.9080	1.8198
0.95	0.05	−0.9222	0.3945	−0.6435	0.6093	0.2804	2.5938	0.9054	1.2559	0.9079	1.8934
1.00	0.00	−0.8989	0.3726	−0.6072	0.5945	0.2811	2.6353	0.9053	1.2625	0.9079	1.9679
				Correlation = −0.8023							

Table 7
Validation test for the average and standard deviation measurements.

Level	i	$f.w.$	Conc.	$f.f$	R_{a1}	R_{a2}	R_{a3}	R_a (μ)	R_a (σ)	R_{t1}	R_{t2}	R_{t3}	R_t (μ)	R_t (σ)
10%	1	0	5	0	0.48	0.60	0.47	0.519	0.072	3.05	3.36	2.57	2.992	0.398
	2	0	10	10	0.58	0.75	0.59	0.643	0.095	3.26	4.52	3.00	3.592	0.813
	3	0	15	20	0.41	0.63	0.46	0.503	0.115	2.46	2.50	2.93	2.629	0.261
	4	0.15	5	10	0.51	0.60	0.51	0.543	0.052	2.72	3.22	2.57	2.836	0.340
	5	0.15	10	20	0.46	0.42	0.47	0.453	0.026	2.38	2.40	3.22	2.666	0.479
	6	0.15	15	0	0.43	0.54	0.51	0.496	0.057	2.39	2.56	4.54	3.162	1.195
	7	0.3	5	20	0.73	0.96	0.60	0.766	0.182	5.62	4.57	3.98	4.722	0.831
	8	0.3	10	0	0.32	0.27	0.21	0.269	0.055	3.14	2.53	2.50	2.722	0.361
	9	0.3	15	10	0.47	0.33	0.43	0.413	0.072	3.86	2.72	3.97	3.516	0.692
LCB								0.351	0.055				2.039	0.403
UCB								0.673	0.157				4.369	1.142
RPD-MNBI								0.434	0.072				3.178	0.453
50%	1	0	5	0	0.08	0.14	0.18	0.133	0.050	1.20	2.25	1.56	1.665	0.534
	2	0	10	10	0.19	0.24	0.27	0.233	0.040	1.85	2.02	2.05	1.969	0.108
	3	0	15	20	0.26	0.32	0.28	0.287	0.031	1.64	3.29	1.92	2.279	0.883
	4	0.15	5	10	0.39	0.42	0.33	0.380	0.046	3.15	2.02	2.73	2.629	0.571
	5	0.15	10	20	0.36	0.41	0.41	0.393	0.029	1.97	2.14	2.44	2.179	0.238
	6	0.15	15	0	0.21	0.37	0.24	0.273	0.085	1.41	2.01	1.79	1.732	0.304
	7	0.3	5	20	0.91	0.72	0.20	0.610	0.368	5.82	6.22	3.16	5.062	1.663
	8	0.3	10	0	0.17	0.19	0.16	0.173	0.015	3.70	3.40	3.16	3.415	0.271
	9	0.3	15	10	0.21	0.17	0.07	0.150	0.072	3.17	3.67	1.65	2.825	1.052
LCB								0.062	0.080				1.804	0.474
UCB								0.524	0.226				4.012	1.345
RPD-MNBI								0.337	0.086				2.425	0.485
90%	1	0	5	0	0.15	0.12	0.28	0.181	0.085	2.40	1.01	1.80	1.732	0.697
	2	0	10	10	0.17	0.32	0.23	0.237	0.075	1.68	1.66	1.62	1.649	0.031
	3	0	15	20	0.24	0.18	0.29	0.234	0.055	2.23	1.51	3.63	2.452	1.078
	4	0.15	5	10	0.30	0.29	0.32	0.301	0.015	3.66	2.72	2.29	2.885	0.701
	5	0.15	10	20	0.10	0.20	0.27	0.187	0.085	0.97	1.50	1.21	1.222	0.265
	6	0.15	15	0	0.18	0.08	0.16	0.137	0.053	1.63	1.08	1.03	1.242	0.333
	7	0.3	5	20	0.59	0.23	0.30	0.371	0.191	4.34	2.23	2.53	3.029	1.142
	8	0.3	10	0	0.26	0.37	0.55	0.391	0.146	2.61	2.80	2.52	2.639	0.143
	9	0.3	15	10	0.14	0.78	0.54	0.484	0.323	2.22	4.68	3.38	3.422	1.231
LCB								0.026	0.088				0.923	0.459
UCB								0.535	0.249				3.582	1.303
RPD-MNBI								0.267	0.131				2.078	0.625

the three scenarios designed in the L9 analysis, the data shown in Table 7 were produced. As expected, the RPD-MNBI method provided not only a robust process but also estimates inside the confidence bounds LCB (lower confidence bound) and UCB (upper confidence bound) for mean and standard deviation.

6. Conclusions and future research

This paper has presented a new approach for robust multi-objective optimization of experiments considering a combination of methods to enable the process to be more resistant to variability. Thus, an application of NBI combined with PCA to a combined array for groups of mean and variance was employed in a finishing end milling operation of AISI 1045 steel. To test the effectiveness of the proposed method, the results of RPD-MNBI were compared to the results of the weighted sums method and the NBI-MSE method.

The hybrid method implemented in this paper generated a low R^2_{Adj}, due to the presence of noise within the control factors. To deal with this issue, the WLS algorithm was implemented for the original responses, R_a and R_t, and for the $PCA_{(RaRt)}$.

Taking the evaluated methods into account, the following findings can be highlighted:

(a) It can be seen that the weighted sums method displayed a series of united points on the Pareto Frontier which complicated the identification of the optimum points.
(b) The NBI-MSE method was, in contrast, able to display a uniform Pareto Frontier.
(c) It was observed that both methods ignored the correlation between responses and led to results that, in practice, were unable to hold up.
(d) The RPD-MNBI method displayed an equally spaced Pareto Frontier in a convex solution region with multiple solutions and gradual trade-offs.
(e) The method considered the correlation structure between responses. As a result it was feasible to perform validation runs to obtain the optimum points identified in the Pareto Frontier.

Three points from the Pareto Frontier were chosen to help prove the ability of the method to mitigate the presence of noise in the process. After determining the power and sample size with a difference of magnitude 0.2 for R_a and R_t responses with a power = 82%, an L9 Taguchi design was used, producing validation runs with 27 samples. The responses were estimated inside the confidence bounds.

This work includes a novel of bi-objective case in which only the first principal component was used. As future work it will be of interest to understand how the inclusion of others controllable variables and the need of more than one principal component will affect the Pareto Frontier shifting the optimum points.

Acknowledgements

The authors would like to express their gratitude to the Brazilian agencies of CNPq, CAPES, and FAPEMIG for their support in this research. Additionally, the authors wish to gratefully acknowledge the referees of this paper, who helped clarify and improve its presentation.

References

Aalae, B. N., Abderrahmane, H., Gael, M., & Olivier, B. (2015). Multicriteria shape design of an aerosol can. *Journal of Computational Design and Engineering, 2*, 165–175.

Ahmadi, A., Moghimi, H., Esmaeel, A. N., Agelidis, V. G., & Sharaf, A. M. (2015). Multi-objective economic emission dispatch considering combined heat and power by normal boundary intersection method. *Electric Power Systems Research*, 32–43.

Bratchell, N. (1989). Multivariate response surface modeling by principal components analysis. *Journal of Chemometrics, 3*, 579–588.

Brito, T. G., Paiva, A. P., Ferreira, J. R., Gomes, J. H. F., & Balestrassi, P. P. (2014). A normal boundary intersection approach to multiresponse robust optimization of the surface roughness in end milling process with combined arrays. *Precision Engineering, 38*(3), 628–638.

Cho, B. R., & Park, C. (2005). Robust design modeling and optimization with unbalanced data. *Computers & Industrial Engineering, 48*, 173–180.

Das, I., & Dennis, J. E. (1998). Normal boundary intersection: A new method for generating the Pareto surface in nonlinear multicriteria optimization problems. *SIAM Journal of Optimization, 8*, 631–657.

Ganesan, T., Vasant, P., & Elamvazuthi, I. (2013). Normal-boundary intersection based parametric multiobjective optimization of green sand mould system. *Journal of Manufacturing Systems, 32*, 197–205.

Gomes, J. H. F., Paiva, A. P., Costa, S. C., Balestrassi, P. P., & Paiva, E. J. (2013). Weighted Multivariate Mean Square Error for processes optimization: A case study on flux-cored arc welding for stainless steel claddings. *European Journal of Operational Research, 226*, 522–535.

Govindaluri, S. M., & Cho, B. R. (2007). Robust design modeling with correlated quality characteristics using a multicriteria decision framework. *International Journal of Advanced Manufacturing Technology, 32*, 423–433.

Hair, J. F., Jr., Black, C. W., Babin, B. J., & Anderson, R. E. (2009). *Multivariate data analysis* (6th ed.). Upper Saddle River, NJ: Prentice Hall. 899 p..

Izadbakhsh, M., Gandomkar, M., Rezvani, A., & Ahmadi, A. (2015). Short-term resource scheduling of a renewable energy based micro grid. *Renewable Energy, 75*, 598–606.

Jeong, I. J., Kim, K. J., & Chang, S. Y. (2005). Optimal weighting of bias and variance in dual response surface optimization. *Journal of Quality Technology, 37*, 236–247.

Johnson, R. A., & Wichern, D. (2007). *Applied multivariate statistical analysis* (6th ed.). New Jersey: Prentice-Hall. 773p.

Kazemzadeh, R. B., Bashiri, M., Atkinson, A. C., & Noorossana, R. (2008). A general framework for multiresponse optimization problems based on goal programming. *European Journal of Operational Research, 189*, 421–429.

Köksoy, O. (2006). Multiresponse robust design: Mean square error (MSE) criterion. *Applied Mathematics and Computation, 175*, 1716–1729.

Kovach, J., & Cho, B. R. (2009). A D-optimal design approach to constrained multiresponse robust design with prioritized mean and variance considerations. *Computers & Industrial Engineering, 57*, 237–245.

Largo, A. R., Zhang, Q., & Vega-Rodríguez, M. A. (2014). A multiobjective evolutionary algorithm based on decomposition with normal boundary intersection for traffic grooming in optical networks. *Information Sciences, 289*, 91–116.

Lee, S. B., & Park, C. (2006). Development of robust design optimization using incomplete data. *Computers & Industrial Engineering, 50*, 345–356.

Lopes, L. G. D., Brito, T. G., Paiva, A. P., Peruchi, R. S., & Balestrassi, P. P. (2016). Experimental design and data collection of a finishing end milling operation of AISI 1045 steel. Data-in-Brief (in press)

Lopes, L. G. D., Gomes, J. H. F., Paiva, A. P., Barca, L. F., Ferreira, J. R., & Balestrassi, P. P. (2013). A multivariate surface roughness modeling and optimization under conditions of uncertainty. *Measurement, 46*, 2555–2568.

Lopez, R. H., Ritto, T. G., Sampaio, R., & de Cursi, J. S. (2014). A new algorithm for the robust optimization of rotor-bearing systems. *Engineering Optimization, 46*(8), 1123–1138.

Montgomery, D. C. (2009). *Design and analysis of experiments* (7th ed.). New York: John Wiley.

Oujebbour, F. Z., Habbal, A., Ellaia, R., & Zhao, Z. (2014). Multicriteria shape design of a sheet contour in stamping. *Journal of Computational Design and Engineering, 1*(3), 187–193.

Paiva, A. P., Campos, P. H., Ferreira, J. R., Lopes, L. G. D., Paiva, E. J., & Balestrassi, P. P. (2012). A multivariate robust parameter design approach for optimization of AISI 52100 hardened steel turning with wiper mixed ceramic tool. *International Journal of Refractory Metals and Hard Materials, 30*, 152–163.

Paiva, A. P., Gomes, J. H. F., Peruchi, R. S., Leme, R. C., & Balestrassi, P. P. (2014). A multivariate robust parameter optimization approach based on Principal Component Analysis with combined arrays. *Computer & Industrial Engineering, 74*, 186–198.

Paiva, A. P., Paiva, E. J., Ferreira, J. F., Balestrassi, P. P., & Costa, S. C. (2009). A multivariate mean square error optimization of AISI 52100 hardened steel turning. *International Journal of Advanced Manufacturing Technology, 43*, 631–643.

Peruchi, R. S., Balestrassi, P. P., Paiva, A. P., Ferreira, J. R., & Carmelossi, M. S. (2013). A new multivariate gage R&R method for correlated characteristics. *International Journal of Production Economics, 144*, 301–315.

Sandvik (2010). Sandvik Coromant catalogue tool.

Shahriari, H., Haji, M. J., & Eslamipoor, R. (2014). An integrated approach for enhancing the quality of the product by combining robust design and customer requirements. *Quality and Reliability Engineering International, 30*(8), 1285–1292.

Shaibu, A. B., & Cho, B. R. (2009). Another view of dual response surface modeling and optimization in robust parameter design. *International Journal of Advanced Manufacturing Technology, 41*, 631–641.

Shin, S., Samanlioglu, F., Cho, B. R., & Wiecek, M. M. (2011). Computing trade-offs in robust design: Perspectives of the mean squared error. *Computers & Industrial Engineering, 60*, 248–255.

Shukla, P. K., & Deb, K. (2007). On finding multiple Pareto-optimal solutions using classical and evolutionary generating methods. *European Journal of Operational Research, 181*, 1630–1652.

Steenackers, G., & Guillaume, P. (2008). Bias-specified robust design optimization: A generalized mean squared error approach. *Computers & Industrial Engineering, 54*, 259–268.

Taguchi, G. (1986). *Introduction to quality engineering: Designing quality into products and processes*. Tokyo: Usian.

Tang, L. C., & Xu, K. (2002). A unified approach for dual response surface optimization. *Journal of Quality Technology, 34*, 437–447.
Vahidinasab, V., & Jadid, S. (2010). Normal boundary intersection method for suppliers' strategic bidding in electricity markets: An environmental/economic approach. *Energy Conversion and Management, 51*, 1111–1119.
Vining, G. G., & Myers, R. H. (1990). Combining Taguchi and response surface philosophies: A dual response approach. *Journal of Quality Technology, 22*, 38–45.
Wu, F. C. (2005). Optimization of correlated multiple quality characteristics using desirability function. *Quality Engineering, 17*, 119–126.
Xu, Z., & Lu, S. (2011). Multiobjective optimization of sensor array using genetic algorithm. *Sensors and Actuators, B: Chemical, 1*, 278–286.
Yuan, J., Wang, K., Yu, T., & Fang, M. (2008). Reliable multiobjective optimization of high-speed WEDM process based on Gaussian process regression. *International Journal of Machine Tools & Manufacture, 48*, 47–60.